Available online at www.sciencedirect.com
ScienceDirect
Nuclear Physics B Proceedings Supplement 00 (2014) 1–7
Nuclear Physics B Proceedings Supplement

The high energy cosmic ray particle spectra measurements with the PAMELA calorimeter

A.V. Karelin[a], O. Adriani[b,c], G.C. Barbarino[d,e], G.A. Bazilevskaya[f], R. Bellotti[g,h], M. Boezio[i], E.A. Bogomolov[j], M. Bongi[b,c], V. Bonvicini[i], S. Bottai[c], A. Bruno[g,h], F. Cafagna[h], R. Carbone[e,i], P. Carlson[k,l], M. Casolino[m], G. Castellini[n], M.P. De Pascale[m,o], C. De Santis[m,o], N. De Simone[m], V. Di Felice[m], V. Formato[i,p], A.M. Galper[a], M.D. Kheymits[a], U. Giaccari[e], S.V. Koldashov[a], S. Koldobskiy[a], S.Yu. Krutkov[j], A.N. Kvashnin[f], A. Leonov[a], V. Malakhov[a], L. Marcelli[o], M. Martucci[o,q], A.G. Mayorov[a], W. Menn[r], M. Merge[m,o], V.V. Mikhailov[a], E. Mocchiutti[i], A. Monaco[g,h], N. Mori[b,c], R. Munini[i,k,l,p], G. Osteria[e], P. Papini[c], M. Pearce[k,l], P. Picozza[m,o], M. Ricci[q], S.B. Ricciarini[c,n], L. Rossetto[k,l], R. Sarkar[i], M. Simon[r], R. Sparvoli[m,o], P. Spillantini[b,c], A. Vacchi[i], E. Vannuccini[c], G.I. Vasilyev[j], G.I. Vasilyev[j], S.A. Voronov[a], Y.T. Yurkin[a], G. Zampa[i], N. Zampa[i], V.G. Zverev[a]

[a] *National Research Nuclear University "MEPHI", RU-115409 Moscow, Russia*
[b] *University of Florence, Department of Physics, I-50019 Sesto Fiorentino, Florence, Italy*
[c] *INFN, Sezione di Florence, I-50019 Sesto Fiorentino, Florence, Italy*
[d] *University of Naples Federico II, Department of Physics, I-80126 Naples, Italy*
[e] *INFN, Sezione di Naples, I-80126 Naples, Italy*
[f] *Lebedev Physical Institute, RU-119991 Moscow, Russia*
[g] *University of Bari, Department of Physics, I-70126 Bari, Italy*
[h] *INFN, Sezione di Bari, I-70126 Bari, Italy*
[i] *INFN, Sezione di Trieste, I-34149 Trieste, Italy*
[j] *Ioffe Physical Technical Institute, RU-194021 St. Petersburg, Russia*
[k] *KTH Royal Institute of Technology, Department of Physics, AlbaNova University Centre, SE-10691 Stockholm, Sweden*
[l] *The Oskar Klein Centre for Cosmoparticle Physics, AlbaNova University Centre, SE-10691 Stockholm, Sweden*
[m] *INFN, Sezione di Rome Tor Vergata, I-00133 Rome, Italy*
[n] *IFAC, I-50019 Sesto Fiorentino, Florence, Italy*
[o] *University of Rome Tor Vergata, Department of Physics, I-00133 Rome, Italy*
[p] *University of Trieste, Department of Physics, I-34147 Trieste, Italy*
[q] *INFN, Laboratori Nazionali di Frascati, I-00044 Frascati, Italy*
[r] *Universitat Siegen, Department of Physics, D-57068 Siegen, Germany*

Abstract

Up until now there has been limited, contradictive data on the high energy range of the cosmic ray electron-positron, proton and helium spectra. Due to the limitations of the use of a magnetic spectrometer, over 8 years experimental data was processed using information from a sampling electro-magnetic calorimeter, a neutron detector and scintillator detectors. The use of these devices allowed us to successfully obtain the high energy cosmic ray particle spectra measurements. The results of this study clarify previous findings and greaten our understanding of the origin of cosmic rays.

Keywords: Cosmic ray; electrons and positrons; protons, helium, calorimeter

1. Introduction

Study of high energy cosmic ray particles in satellite experiments is one of the main tasks in modern astrophysics. Cosmic ray electrons with energy more than 10 GeV carry important information about their origin and propagation through interstellar space. The energy spectra of cosmic ray electrons is known to be

affected by the inverse inverse Compton effect, synchrotron emission and possible dark matter particles. During propagation the time of energy losses for 1 TeV electron is about 10^5 years corresponding to 1 kps. Due to these significant energy losses the electrons are not able to cover distant areas from their sources. The direct measurement of positron and electron spectra in cosmic ray with satellites in space should help to improve existent models as well as create a new one that describes the processes of electron-positron generation and propagation. Today just 3 satellites are taking measurements of electron-positron fluxes - they are Fermi [1], AMS-02 [2] and PAMELA [3]. In ground based experiments (HESS [4], Kabayashi et al. [5]) the abrupt falling or cutoff in the electron-positron spectrum have been demonstrated at energies higher than few hundred GeV. But resent satellite experiments Fermi [6] and AMS-02 [7, 8] do not show this behaviour.

Up to now experimental results of proton and helium energy spectra measurements agree that proton and helium spectrum slopes are different [9, 10, 11, 12, 13, 14], that became more obvious in TeV region, but different experiments disagree in the value of this difference. Regardless of the value of the difference, the nature of such a difference remains unknown.

The use of a calorimeter would extend the measured energy range in the PAMELA experiment. Thus allowing for the clarification of previous studies.

2. The PAMELA experiment

The PAMELA experiment was put into space on board of the Resurs DK1 satellite from the Baikonur Cosmodrome on June 2006. It was designed to study the composition and energy spectra of cosmic ray particles in a wide energy range in near-Earth space. The PAMELA instrument (a total mass is 470 kg) consists of several specialized detectors as shown in Fig.1: a permanent magnet equipped with the silicon tracking system, a time of flight (ToF) system made of three double planes, anticoincidence counters, a neutron detector (ND), a bottom shower scintillator detector and a tungsten/silicon sampling electromagnetic calorimeter.

The sensitive elements in the ND [15] are the He^3 neutron counters 18.5 mm in diameter and 200 mm sensitive length. The counters recording neutrons by a reaction $He^3 + n \longrightarrow H^3 + p$ are mainly sensitive to the thermal neutrons (cross section more than 5000 barns). Two layers of 18 counters (36 pieces in total) are placed into the polyethylene moderator. One polyethylene block 2 g/cm^2 thick is above the upper layer of counters, similar block is between the upper and the bottom layer of

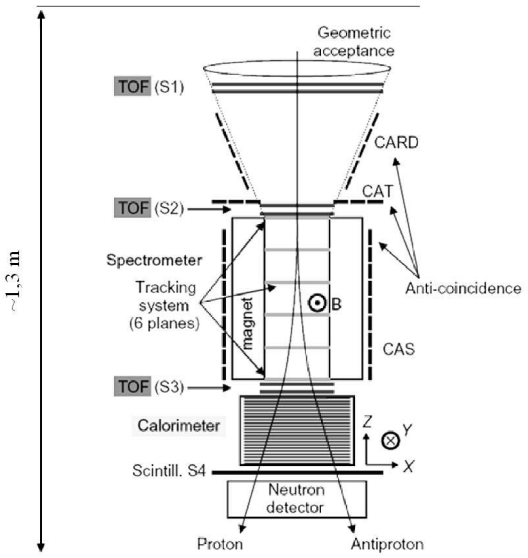

Figure 1: The PAMELA instrument.

counters, and 6 g/cm^2 of polyethylene are beneath. The Cd shield 0.5 mm in thickness envelopes the ND from the bottom and the sides. The ND is mounted under the S4 scintillator.

The total calorimeter [16] thickness is 16.3 radiation lengths and 0.6 nuclear interaction length. The calorimeter is composed of 44 silicon layers (SSD)interleaved by 22 tungsten plates with a thickness of 0.26 cm thick. Each silicon plane is 380μm thick and segmented in 96 strips with a pitch of 2.4 mm. 22 planes are used for the X view and 22 for the Y view in order to provide topological and energetic information about the showers produced inside the calorimeter. The ToF system [17] comprises six layers of fast plastic scintillators arranged in three planes (S1, S2 and S3). Each detector layer is segmented into strips, placed in alternate layers orthogonal to each other. The distance between S1 and S3 is 77.3 cm.

The magnetic spectrometer allows the energy of incident protons and helium nuclei to be precisely measured up to about 1 TeV/nucleon while the energy of electrons up to 600 GeV. However, the measurements of the spectra can be extended to higher energies by using the calorimeter information.

3. The method for electron-positron spectrum measurement

The electron-proton separation method for the calorimeter depends on an incident angle. It has been

chosen to select just particles that cross the calorimeter straight down with a small deviation angle. It provides a better energy resolution and suppresses a proton background more efficiently due to the fact that the major fraction of a shower is contained inside the calorimeter. The main part of these particles came within the main aperture while another part penetrates through the magnetic system (the magnet and its surrounding electronics). If a particle generates the shower inside the magnet (it is rather thick in terms of nuclei lengths and all electrons in case of crossing it generate showers) the calorimeter registers only a part of the shower. In the latter such particles have to be excluded from further consideration (see below).

The presented method is based on the GEANT3 simulation code that has been adapted to PAMELA detectors. The GEANT3 simulation has been used to estimate the values of parameters corresponding to protons and electrons.

The first step as the basic cut was the threshold for a total energy release inside the calorimeter - Etot. Such criterion allows the extraction of the events corresponding to the high energy particles generating the shower inside the calorimeter. The certain amount of energy release does not correspond to the same values of primary energies for protons, electrons and nuclei. The certain energy release could correspond to certain values of electron energy or few times higher proton energy as well. Thus it is sufficient to notice here that proton events have been simulated in the wide energy range up to 15 TeV as these energy protons still contribute to the contamination of 300-3000 GeV electrons.

A shower axis reconstruction procedure, which defines the primary particle direction inside the calorimeter, is a crucial stage of the electron-proton separation method. In this method all parameters used are closely related to the shower axis. Therefore the next selection criterion was the sampling of events that had a easily recognisable track inside the calorimeter. Otherwise if there were no tracks the events were discarded. Most likely is that the last type of events has been generated by particle interaction with the Pamela magnet system or with the structure of the satellite and these primary particles have not penetrated the calorimeter. The direction reconstruction algorithm consists of multi-step resolution of a shower axis equation. The precise description of the procedure can be located at [18]. The parameter RMS (root mean square) associated with a lateral development of the shower. RMS represents the root-mean-square deviation of energy release at some distances from energy release directly at the shower axis. RMS indicates the transversal density of the shower inside the calorimeter and is defined by:

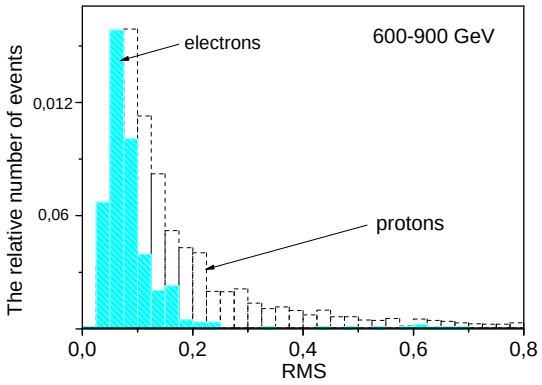

Figure 2: The distribution of RMS deviations for the second subset of the calorimeter planes. The simulation data.

$$RMS_l^2 = \frac{\sum\limits_i E_l^i (X_i - X_l^c)^2}{\sum\limits_i E_l^i}, \quad (1)$$

where l - the number of the calorimeter plane, i - the plane strip number, E - the energy release, X^c - the shower axis coordinate, X - the strip coordinate. The value of RMS depends on the shower shape in the certain calorimeter. In the case of the PAMELA calorimeter, E_l^i has to be squared, which corresponds to the simulation results of the electromagnetic interaction inside the PAMELA calorimeter. This criterion was applied in the ATIC balloon borne experiment, where it became the basis of the procedure of electron separation from protons [19].

However, the RMS criterion appear to be inefficient for the first planes of the PAMELA calorimeter. For a significant fraction of particles, the shower generation begins in these planes, so an electromagnetic cascade is not developed fully. This conclusion is valid for the first ten planes of 44. In the case of shower generation in the first planes of the calorimeter, the set of the remaining planes was broken down into three subsets corresponding to different parts of the electromagnetic shower. These subsets include planes from the 11th to the 20th (increment of shower), the 21st to 30th (shower-development maximum) and the 31st to 44th (decrement of shower), respectively. Figure 2 shows the proton and electron distribution of RMS deviations for the second subset of planes with the energy deposition values corresponding to electron energy ranges 600-900 GeV.

The longitudinal development of the shower is also important to separate electrons from protons. A lon-

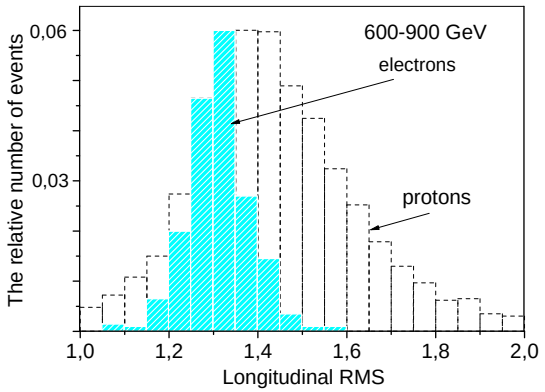

Figure 3: The longitudinal RMS distribution. The simulation data.

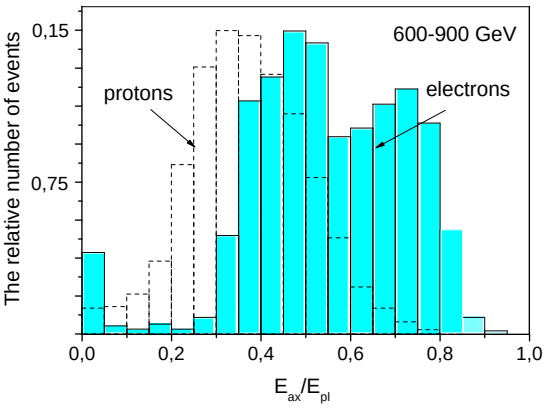

Figure 4: The distribution of ratio E_{ax}/E_{pl}, where E_{ax} - the energy release along the shower axis for plane 2, E_{pl} - the energy release in plane 2. The simulation data.

gitudinal RMS calculation is similar to the lateral one. The strips are changed on the planes while the summation is done within the whole calorimeter with a similar equation. The longitudinal RMS distributions for protons and electrons are shown in fig 3.

Energy release along the shower axis is another separation criterion. According to Molier shower development theory, 90 % of the shower energy is concentrated within 1 Molier radius around the shower axis. This parameter has been used for different planes of the calorimeter. The distribution of this parameter for plane 2 for electron energy ranges 600-900 GeV is shown in fig 4. A double peak can be seen in the electron distribution. The left peak corresponds to particles that generate the shower somewhere above the calorimeter (mentioned above). So by installing a special threshold for energy release along the shower axis it is possible not only to cut a part of protons but to reject electrons from the left peak as well.

The figures 2,3,4 allow the conclusion that the final samples of the selected events are not pure electrons. It means that if one would like to reconstruct the real electron spectrum it is important to estimate the proton background in each energy bin in the electron spectrum. It has been done by using the proton spectrum that had been measured in PAMELA experiment by the calorimeter (see [9]).

With this spectrum the amount of protons N in each electron spectrum bin has been calculated according to the formula:

$$N_p(E_1 \div E_2) = \int_{E_1}^{E_2} F(E) G \varepsilon(E) \Delta t dE, \qquad (2)$$

where E_1 and E_2 the minimum and maximum electron energies in the bin, respectively, F(E) energy spectrum according to [9], G is geometric factor, ε(E) is the relative number of survived proton obtained from GEANT3 simulation, Δt is exposure.

Unfortunately at high energies in the last two bins that cover energy range 900-3000 GeV the fraction of protons is too high to make it possible to achieve reliable results for the electron spectrum. For these bins the ND data has been used additionally. On fig 5 one can see the neutron distributions for electron energy ranges 600-900 GeV. The number of the neutrons equal to 8 has been chosen to separate two areas: 1) the mixture of electron and protons (less than 8 neutrons) and 2) only protons (more than 8 neutrons). However at the range 1500-3000 GeV due to the lack of a statistic it was possible just to install an upper limit for the electron spectrum.

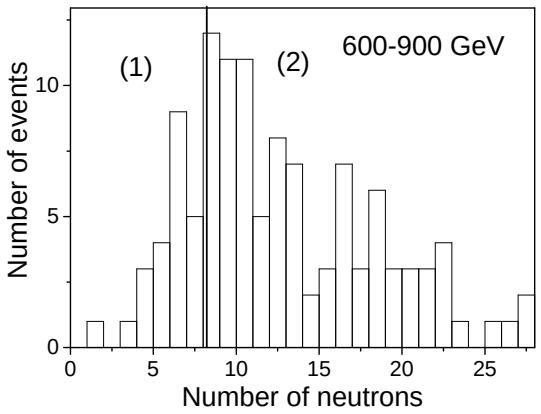

Figure 5: The neutron number distributions.The experimental data.

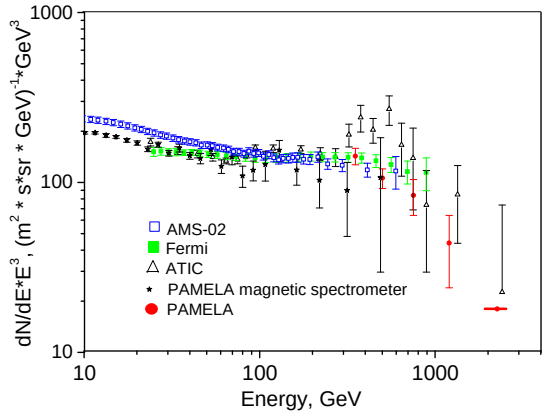

Figure 6: The obtained electron-positron spectrum in compare with direct measurements.

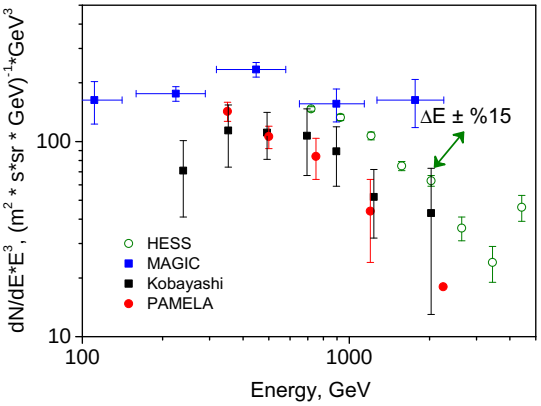

Figure 7: The obtained electron-positron spectrum in compare with ground-based measurements.

The total amount of electrons has been calculated in each energy bin after subtraction of the proton background. The events have been taken for a time period covered 2009-2013 years in the experimental data set. To calculate the electron energy spectrum the number of selected events has to be divided by an exposure that was equal to 116006101,7 s. In the end a nuclei contamination has been estimated by using the scintillator detectors of the ToF system. Among these events no particle with the a charge of more than 1 has been found. Therefore one can make a conclusion that selected events do not contain a significant nuclei contribution. Thereby the helium contamination could be neglected. The geometric factor was calculated within a wide aperture by GEANT3 code. The energy of electrons was obtained by measurements of total energy released inside the calorimeter.

4. The results of electron-proton spectrum measurements

The presented results are compared with spectra from the other experiments: ATIC-2 [20], AMS-02 [7], Fermi [6], the single electron spectrum obtained with the magnetic spectrometer of the PAMELA instrument [21] on fig 6 and with HESS[4], Magic[22] and Kobayashi[5] on fig 7.

The error bars include only statistical uncertainties. The last point indicates an upper limit for 1500-3000 GeV measurements. If one takes into account the energy measurement uncertainty of 15 % in HESS results then a conclusion is that the PAMELA results correspond more to ground based measurements HESS and Kobayashi than satellite ones - AMS-02 and Fermi. PAMELA results demonstrate a clear spectrum fall after few hundred GeV while it looks like another two satellite measurements do not show any significant decline with energy increasing.

5. The method for proton and helium spectra measurement

The method for proton and helium spectra measurements is similar to the previous one [9]. However the main stress was made for energies more than 1 TeV to increase statistics at these energies as much as possible. As such energies were considered the special selection cut for electrons was no longer needed. Indeed, according to the Monte-Carlo simulation after 1 TeV energy the contribution of electrons to protons is negligible. The events were collected in a wide aperture as it was allowed by size of ToF system scintillator detectors. All together along with the doubling exposure time allowed to increase statistics for protons by 5 times.

The helium nuclei were distinguished according to the charge which was measured by ionization losses in scintillators. So for helium, the problem of electron suppression does not exist. The statistic was increased by 3 times, due two remaining factors. Nevertheless the new measurements at higher energies up to 10 TeV/nuclon within two last bins were achieved.

6. The results of proton and helium spectra measurements

The presented results are compared with spectra from the other experiments: ATIC-2 [11], AMS-02 [13, 14] - fig 8., CREAM [12] and the spectrum measured with the magnetic spectrometer of the PAMELA instrument [10]

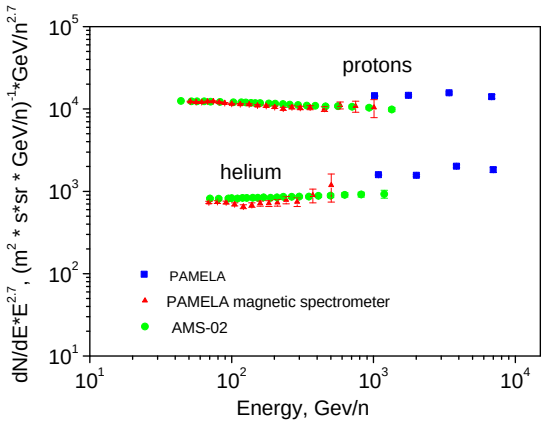

Figure 8: The obtained proton and helium spectra in compare with AMS-02 and magnetic spectrometer PAMELA results.

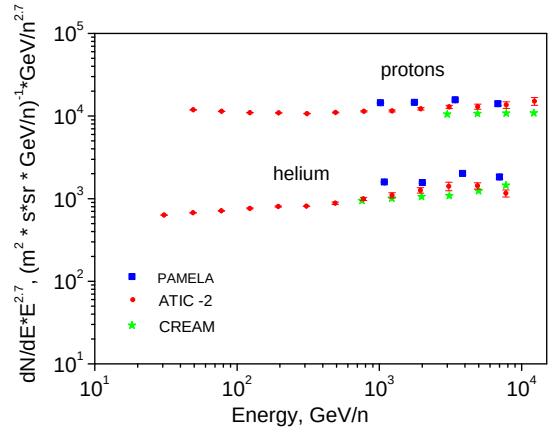

Figure 9: The obtained proton and helium spectra in compare with ATIC-2 and CREAM results.

on fig 9. The error bars include only statistical uncertainties. The results of this study are in general agreement with others. Nevertheless the PAMELA calorimeter data are systematically higher. Thus it is proved that spectra of protons and helium nuclei have different slope indexes throughout the entire energy range, but at high-energies the difference becomes less significant. The spectrum increase of helium nuclei in the magnetic spectrometer PAMELA data more corresponds to results obtained by using the PAMELA calorimeter than the results of the AMS-02.

7. Conclusion

Due to the use of the calorimeter in assistance with scintillators and ND defectors the high energy range was achieved in the measurements of the electron-positron, proton and helium spectra. The results of measurements of the electron-positron spectrum demonstrate the fall after 300 GeV that corresponds to the ground based cherenkov and emulsion chamber experiments while the other satellite measurements do not demonstrate a clear cutoff at these energies.

The increased statistics allowed the energies, which were not available before in direct measurements of cosmic ray helium spectrum, to be reached.The difference between the slope of proton spectrum and the one of the helium spectrum was confirmed as well as the change of helium slope spectrum index in the 100-10 TeV/n region. All of this finding helps with new understanding of the processes of acceleration and prorogation of primary cosmic rays in the Galaxy.

We are grateful to the Russian Science Foundation grant (14-12-00373) and the President of the Russian Federation (grant MK-4599.2014.2) for support.

References

[1] A. A. Abdo, et al., Measurement of the cosmic ray $e^- + e^+$ spectrum from 20 GeV to 1 TeV with the Fermi large area telescope, Phys. Rev. Lett. 102 (2009) 181101.
[2] F. Palmonari, et al., Search for dark matter in cosmic rays with the AMS-02 space spectrometer, Journal of Physics: Conference Series 335 (2011) 012066.
[3] P. Picozza, et al., Pamela - a payload for antimatter matter exploration and light-nuclei astrophysics., Astropart. Phys. 27 (2007) 296.
[4] F. Aharonian, et al., Energy spectrum of cosmic-ray electrons at TeV energies, Phys. Rev. Lett. 101 (2008) 261104.
[5] T. Kobayashi, Y. Komori, K. Yoshida, N. J., The most likely sources of high-energy cosmic-ray electrons in supernova remnants, Atrophys. J. 601 (2004) 340.
[6] M. Ackermann, et al., Fermi LAT observations of cosmic-ray electrons from 7 GeV to 1 TeV, Phys. Rev. D 82 (2010) 092004.
[7] B. Bertucci, Precision measurement of the electron plus positron spectrum with AMS, in: Proceedings of the 33rd ICRC, 2013.
[8] Z. Weng, V. Vagelli, AMS-02 measurement of cosmic ray positrons and electrons, in: ICHEP, 2014.
[9] O. Adriani, et al., Measurements of cosmic-ray proton and helium spectra with the PAMELA calorimeter, Adv. Sp. Res. 51 (2013) 219.
[10] O. Adriani, et al., PAMELA measurements of cosmic-ray proton and helium spectra, Science 232 (2011) 69.
[11] A. Panov, et al., Energy spectra of abundant nuclei of primary cosmic rays from the data of ATIC-2 experiment: Final results, Bulletin of the Russian Academy of Sciences: Physics 73 (2009) 564.
[12] H. Ahn, et al., Discrepant hardening observed in cosmic-ray elemental spectra, ApJ Lett. 714 (2010) 89.
[13] S. Haino, Precision measurement of the proton flux with AMS, in: Proceedings of the 33rd ICRC, 2013.

[14] V. Choutko, Precision measurement of the cosmic ray helium flux with AMS experiment, in: Proceedings of the 33rd ICRC, 2013.
[15] Y. Stozhkov, The in-flight performance of the PAMELA neutron detector., in: Proceedings of the 30th ICRC, Vol. OG1, 2007, p. 325.
[16] M. Boezio, et al., A high granularity imaging calorimeter for cosmic-ray physics, Nucl. Instrum. Meth. A 487 (2002) 407.
[17] G. Osteria, et al., The tof and trigger electronics of the PAMELA experiment., Nucl. Instrum. Meth. A 518 (2004) 161.
[18] A. Karelin, et al., Reconstructing the particle direction in an extended aperture of the PAMELA apparatus using the coordinate-sensitive calorimeter, Instruments and Experimental Techniques 56 (2013) 1.
[19] J. Chang, et al., Resolving electrons from protons in ATIC, Adv. Sp. Res. 42 (2008) 431.
[20] J. Chang, et al., An excess of cosmic ray electrons at energies of 300800 GeV, Nature 456 (2008) 362.
[21] O. Adriani, et al., Cosmic-ray electron flux measured by the PAMELA experiment between 1 and 625 GeV, Phys. Rev. Lett. 106 (2013) 201101–01–05.
[22] D. B. Tridon, A study of cosmic electrons between 100 GeV and 2 TeV with the magic telescope, Ph.D. thesis, Technische Universitat Munchen (2011).